The C-Terminal Region of Human Glutathione Transferase A1-1 Affects the Rate of Glutathione Binding and the Ionization of the Active-Site Tyr9†

Ann Gustafsson, Maryam Etahadieh, Per Jemth, and Bengt Mannervik*

Department of Biochemistry, Uppsala University, Biomedical Center, Box 576, S-751 23 Uppsala, Sweden

Received June 28, 1999; Revised Manuscript Received October 5, 1999

ABSTRACT: In human glutathione transferase (GST) A1-1, the C-terminal region covers the active site and contributes to substrate binding. This region is flexible, but upon binding of an active-site ligand, it is stabilized as an amphipatic α-helix. The stabilization has implications for the catalytic activity of the enzyme. In the present study, residue M208 in GST A1-1 has been mutated to Lys and Glu, and residue F220 to Ala and Thr. These mutations are likely to destabilize the C-terminal region due to loss of hydrophobic interactions with the rest of the hydrophobic binding site. The rate constant for binding of glutathione to wild-type GST A1-1 is 450 mM^{-1} s^{-1} at 5 °C and pH 7.0, which is less than for an association limited by diffusion. However, the M208 and the F220 mutations increase the apparent on-rate constant for glutathione binding to 640−1170 mM^{-1} s^{-1}. The binding data can be explained by a rapid reversible transition between different enzyme conformations occurring prior to glutathione binding, and restriction of the access to the active site by the C-terminal region. The effect of the mutations appears to be promotion of a less closed conformation, thereby facilitating the association of glutathione and enzyme. Both the M208 and F220 mutants display a lowered pK_a value (≈0.3 log unit) of the catalytically important Tyr9. Residue 208 does not interact directly with Tyr9 in the active site, and the shift in pK_a value is therefore ascribed to the proposed dislocation of the C-terminal region caused by the mutation.

The glutathione transferases (GSTs)[1] are a family of detoxication enzymes that protect the living cell from a wide range of environmentally and endogenously produced electrophilic compounds. The electrophilic substrates are largely nonpolar. The GSTs conjugate the thiol group of the tripeptide glutathione (γ-Glu-Cys-Gly) to the electrophilic center. The electrophile is thereby rendered harmless, and its water solubility is increased, promoting degradation of the product and subsequent excretion from the organism. The soluble mammalian GSTs are divided into a number of classes (*1*−*6*) mainly based on their primary structures. The classes are named Alpha, Kappa, Mu, Pi, Sigma, Theta, and Zeta. The sequence identities within a class are greater than 50%, but between different classes, they are significantly lower. Despite the divergent sequences, the structural scaffold of the amino acid backbone has been well preserved during evolution. All soluble GSTs have a dimeric structure in which each subunit is divided into two distinct domains. The N-terminal domain forms the glutathione binding site (G-site). The C-terminal domain and parts of the N-terminal domain build up the hydrophobic substrate binding site (H-site).

Extensive studies of the glutathione transferases have shown that a conserved N-terminally located tyrosine residue plays an important role in the action of the Alpha, Mu, and Pi class isoenzymes (*7*−*22*). It is generally concluded that the tyrosine hydroxyl group activates the thiol group of glutathione by donating a hydrogen bond, thereby stabilizing the deprotonated and nucleophilic form of the tripeptide (*8*, *10*, *12*, *15*, *17*−*19*, *22*). In human and rat GST A1-1, the catalytically important tyrosine is located at position 9, and the pK_a values of the phenolic hydroxyl group are very low, 8.1 and 8.4, respectively (*13*, *17*).

The greatest divergence among the classes is found in the H-site of the proteins where evolution has made the different isoenzymes capable of binding substrates with different characteristics (*23*). One of the structural features separating the Alpha class enzymes from the GSTs of other classes is a C-terminal α-helix (residues 210−220) that forms a cap over the active site (*24*). The C-terminal region is flexible, and both a crystallographic analysis (*25*) and an NMR study (*26*) have shown that the structural order is highly dependent on the occupancy of the two binding pockets of the active site (Figure 1). In the crystal structure of the apo-enzyme, where neither the G-site nor the H-site is occupied, only traces of electron density associated with the helix can be detected. The C-terminal helix is stabilized when the G-site and the H-site are engaged in ligand binding, as in the complex with *S*-benzylglutathione (*24*). In agreement with this, the NMR studies show that the intensity of the signal corresponding to Phe220, located in the C-terminus (Figure 1), is dependent on the absence or presence of glutathione and the hydrophobic substrate 1-chloro-2,4-dinitrobenzene (CDNB). Moreover, the chemical shift of the resonance from the C-terminal amino acid, Phe222, is altered upon substrate binding, indicating structural changes in the C-terminus of the protein (*26*).

† This work was supported by grants from The Swedish Natural Science Research Council.

* Address correspondence to this author at the Department of Biochemistry, Uppsala University, BMC, Box 576, S-751 23 Uppsala, Sweden. Telephone: (+46) 18-4714539. FAX: (+46) 18-558431. E-mail: Bengt.Mannervik@biokem.uu.se.

[1] Abbreviations: CDNB, 1-chloro-2,4-dinitrobenzene; G-site, glutathione binding site; GSH, glutathione; GST, glutathione transferase; H-site, hydrophobic substrate binding site.

10.1021/bi991482y CCC: $18.00
Published on Web 11/17/1999

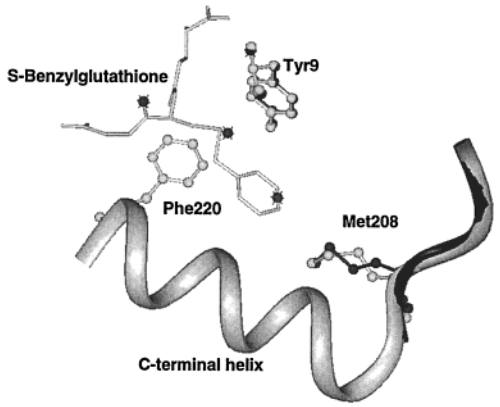

FIGURE 1: Representation of the active-site structure of GST A1-1. The structure of the apoform of GST A1-1 (*25*), in black, is superimposed on the structure of GST A1-1 in complex with *S*-benzylglutathione (*24*), in light gray. The C-terminal α-helix cannot be seen in the apo-enzyme since the large mobility in this part of the enzyme does not allow any structural determination. The side chains of Tyr9, Phe220, and Met208 are displayed in a ball-and-stick mode. *S*-Benzylglutathione is displayed in stick mode. Tyr9 essentially retains its conformation upon ligand binding while the side chain of Met208 shows a larger change in structure. The shortest distance between these two side chains is approximately 7.5 Å. The three active-site water molecules located closest to the hydroxyl group of Tyr9 in the apo-enzyme structure are shown. The distances between the oxygen of the hydroxyl group and the oxygens of the water molecules are 2.8, 4.8, and 7.1 Å. All three water molecules are displaced when *S*-benzylglutathione occupies the active site.

Phe220 is one of four hydrophobic amino acids in the C-terminal helix that directly contributes to the active site (Figure 1). In the 3-dimensional structure, Phe220 points toward the aromatic face of Tyr9 (Figure 1). Phe220 mutants of rat GST A1-1 have been studied (*27*, *28*), and, in addition to affecting the stability of the C-terminus, alterations in position 220 modify the apparent pK_a value of the catalytically active Tyr9. One of the conclusions drawn from these experiments was that a more structured and closed conformation of the C-terminal helix results in a lower pK_a value for Tyr9.

The present study is based on two previous studies of human GST A1-1 mutants (*29*, *30*) where the H-site amino acid Met208 was substituted by Lys (M208Kh)[2] and Glu (M208E). Residue Met208, immediately preceding the C-terminal helix (Figure 1), is located in the H-site of GST A1-1. Both M208Kh and M208E display a marked decrease in catalytic efficiency (*29*, *30*). The enhanced polarity in the H-site of M208Kh and M208E presumably disrupts the hydrophobic interactions with the H-site-facing part of the amphipatic C-terminus, changing its structure toward a more open and less structured conformation. The lost activity of the M208Kh mutant is regained in the presence of benzoic acid derivatives. The best activator of M208Kh, 4-propylbenzoic acid, affords a total recovery of the lost activity (*30*), probably by neutralizing the positive charge introduced at position 208. The reestablishment of hydrophobic interactions between the substrate and the C-terminus is thereby promoted.

The two M208 mutants have now been used to investigate how the C-terminal region affects the ionization of Tyr9 and the binding and activation of glutathione. For comparison, Phe220, known to affect helix stability (*28*), has been mutated to Ala and Thr.

EXPERIMENTAL PROCEDURES

Construction, Expression, and Purification of the GST A1-1 Variants. F220A and F220T were constructed by PCR-based site-directed mutagenesis using the forward primer (Amersham Pharmacia Biotech, Uppsala, Sweden) 5′-AAA-AAA*GAATTC***CATATG**GCAGAGAAGCCCAAGCTCCAC-3′. The italicized letters indicate an *Eco*RI site, and the boldface letters are an *Nde*I site. The reverse mutagenic oligonucleotide primer (Amersham Pharmacia Biotech) has the following sequence: 5′-ACGCGTCGACTTAAAAC-CTAGYSSTCTTCCTTGCTTC-3′. The underlined letters encode a *Sal*I site, and Y marks C or T. The PCR contained 10 ng of pGΔETacA1 (*29*) as template DNA, 0.2 mM dNTPs, 1.5 μM of each primer, 2.5 units of *Taq* DNA polymerase (Fermentas AB, Vilnius, Lithuania), 10 mM Tris-HCl (pH 8.8), 50 mM KCl, and 1.5 mM $MgCl_2$. The PCR was conducted using the following temperature cycle: 95 °C for 1 min, 55 °C for 2 min, 72 °C for 2 min repeated 30 times followed by 10 min at 72 °C. The PCR product was digested with *Sal*I and *Eco*RI and ligated into pGEM-3Z (Promega Co., Madison, WI). *Escherichia coli* XL1-Blue cells (Stratagene, La Jolla, CA) were transformed with the ligation mixture by electroporation. Positive clones were identified by blue/white selection. The mutant clones, pGF220A and pGF220T, were confirmed by DNA sequence analysis (*31*). pGF220A and pGF220T were digested with *Nde*I and *Sal*I, and the fragments obtained were subcloned into pET21-a (Novagen, Inc., Madison, WI) and used for transformation of *E. coli* BL-21 (Novagen). The construction of the expression vectors encoding M208Kh and M208E has previously been described (*29*, *30*). The enzymes were expressed and purified using HiTrap SP cation exchange as described by Gustafsson and Mannervik (*30*). All enzymes were >95% pure as judged from an SDS−PAGE gel (*32*).

Enzymatic Assays. The specific activity and the steady-state kinetics with CDNB as the electrophilic substrate (*33*) were measured with F220A and F220T as earlier described (*30*).

Preequilibrium Binding of Glutathione. All stopped-flow experiments were carried out on an SX.18MV Sequential Stopped-flow Spectrometer (Applied Photophysics Limited, Leatherhead, U.K.). Binding of glutathione to the wild-type GST A1-1 was studied in two ways: by following quenching of the intrinsic fluorescence of the enzyme, using an excitation wavelength of 280 nm; and by measuring the change in absorbance at 239 nm, indicating the deprotonation of glutathione (*34*). Mixing 50 μL of GST A1-1 with 50 μL of glutathione gave a final concentration of GST A1-1 subunits of 15−30 μM. The glutathione concentration was varied between 0.1 and 3 mM, and the assay buffer was 0.1 M sodium phosphate (pH 6.0−7.25). To decrease the binding rate to measurable velocities, the experiments were conducted at 5 °C. k_{obs} was obtained by fitting a single-exponential

[2] Names of GST A1-1 mutants: F220A, phenylalanine 220 mutated to alanine; F220T, phenylalanine 220 mutated to threonine; M208K, methionine 208 mutated to lysine; M208Kh, M208K containing a 6-histidine tag in the N-terminus; M208E, methionine 208 mutated to glutamic acid.

equation to the data using the program supplied by the manufacturer.

Preequilibrium binding of glutathione to rat GST T2-2 at 4 °C was studied as described previously (*35*).

Binding of glutathione to M208Kh, F220A, and F220T was measured by monitoring the deprotonation of glutathione at 239 nm. The experiments were conducted as described above with some exceptions: the concentration of enzyme was between 30 and 60 μM subunits; 75 μL of enzyme and 75 μL of glutathione solutions were mixed in each shot. The glutathione concentration was varied between 0.08 and 0.5 mM.

Determination of pK_a for Tyr9 and for Enzyme-Bound Glutathione. The ionization of Tyr9 in the active site of the different GST A1-1 variants was measured by difference spectroscopy on a UV-2501PC Shimadzu spectrophotometer (Shimadzu Scientific Instruments, Inc., Columbia, MD) using 0.1 M sodium phosphate at pH 4.0−8.0 and 0.1 M ethanolamine/HCl at pH 8.5−9.0 at 22 °C. The protein concentrations were between 7 and 15 μM subunits. Difference spectra of the GST A1-1 variants were recorded between 220 and 360 nm both in the absence and in the presence of 0.5 mM glutathione (wild-type and M208 mutants) or 2 mM glutathione (F220 mutants). In the case of M208Kh, measurements were also conducted in the presence of 1.5 mM 4-propylbenzoic acid. When the pK_a value of Tyr9 was determined, the spectrum at pH 5.5 (wild type and F220 mutants) or at pH 5.0 (Met208 mutants) was subtracted from the other spectra. The peaks arising at 298−301 and 250−255 nm were used to monitor tyrosinate formation. The pK_a value was calculated from the peaks obtained by plotting the tyrosinate concentration per enzyme subunit, using a $\Delta\epsilon_{300}$ of 2350 M^{-1} cm^{-1} and a $\Delta\epsilon_{253}$ of 11 000 M^{-1} cm^{-1} (*13*, *17*, *27*), against pH. The equation $\Delta A = \Delta A_{max}/[1 + 10^{(pK_a - pH)}]$ was fitted to the data using GraphPad Prism.

The pK_a of the sulfhydryl group of glutathione was determined from spectra where 0.5 or 2 mM tripeptide was present in the sample cuvette. To obtain difference spectra, the spectra for the enzyme alone (at pH 5.0 or pH 5.5) and glutathione alone (at the different pH values) were both subtracted from the spectrum of the binary enzyme−glutathione complex. The pK_a of active-site-bound glutathione was calculated from the peak obtained at 239 nm [$\Delta\epsilon_{239} = 5200$ M^{-1} cm^{-1} (*27*, *34*, *36*)].

RESULTS

Kinetic Properties of the F220 Mutants. The steady-state kinetic properties of the F220 mutants were characterized by measuring the specific activities and saturation curves with CDNB. Results are presented in Table 1. The limited solubility (approximately 2 mM) made it impossible to raise the CDNB concentration to saturating levels, resulting in low precision of K_m^{CDNB} and k_{cat}. The catalytic efficiencies, k_{cat}/K_m^{CDNB}, of the F220 mutants are lower than that of the wild-type GST A1-1 and similar to the constants obtained for M208Kh and M208E (*29*, *30*). It seems as if the catalytic efficiencies are reduced mainly due to an increase of K_m^{CDNB} as compared to the wild-type data.

Preequilibrium Binding of Glutathione. The pH dependence of the preequilibrium binding of glutathione to the wild-type GST A1-1 was studied by following the quenching of the intrinsic fluorescence and by monitoring the active-site ionization of glutathione at 239 nm. To investigate how the proposed increased flexibility of the C-terminus affected glutathione binding, the preequilibrium kinetics of M208Kh and the F220 mutants were determined. The fluorescence quenching of M208Kh and the F220 mutants did not give signals strong enough to determine any rate constants. Thus, only data from active-site ionization of the tripeptide could be used for comparison with the wild-type data. The binding constants for rat GST T2-2 have earlier been determined at 15 °C (*35*). In the present study, k_{on} and k_{off} for rat GST T2-2 were measured at 4 °C to get constants comparable to those obtained for GST A1-1. All experimental traces were well described by a single-exponential curve from which the observed rate constant, k_{obs}, could be derived.

Table 1: Kinetic Properties of the Wild-Type and Mutant Forms of GST A1-1[a]

enzyme	k_{cat} (s^{-1})	K_M^{CDNB} (mM^{-1})	k_{cat}/K_M^{CDNB} (s^{-1} mM^{-1})	sp act. (μmol min^{-1} mg^{-1})
wild type	88 ± 3[b]	0.56 ± 0.04[b]	160 ± 8.0[b]	75[c]
F220A	120 ± 40	7 ± 3	18 ± 1	14
F220T	280 ± 150	13 ± 8	22 ± 1	24
M208Kh	−[e]	−	8.3 ± 0.9[d]	12[d]
M208E	−	−	2.6 ± 0.4[d]	6.0[d]

[a] Parameter values and their standard deviation were obtained by nonlinear regression analysis. [b] From Widersten et al. (*29*). [c] From Björnestedt et al. (*17*). [d] From Gustafsson and Mannervik (*30*). [e] (−) Data could not be obtained.

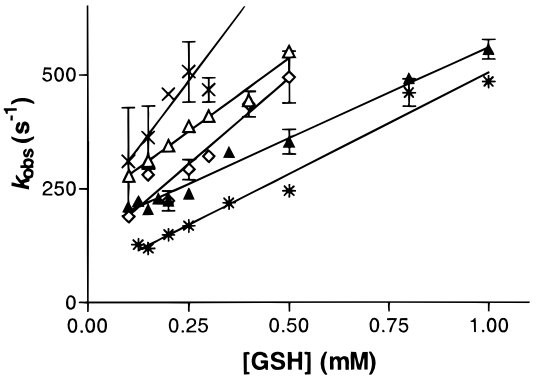

FIGURE 2: Preequilibrium kinetics of glutathione binding to the active site of wild-type GST A1-1, M208Kh, F220A, and F220T were monitored by following the active-site ionization of glutathione as the increase in absorbance at 239 nm (at 4 °C). The observed rate constant is plotted versus glutathione concentration. k_{on} and k_{off} are obtained from the relationship: $k_{obs} = k_{on}[GSH] + k_{off}$. (▲) Wild-type enzyme, pH 6.5; (*) wild type, pH 7.0; (◇) M208Kh, pH 7.0; (×) F220A, pH 7.0; (△) F220T, pH 7.0.

The data obtained from the measurements (Figure 2, Table 2) may be described by Scheme 1. The first step is a rapid equilibrium between two or more different enzyme conformations where glutathione binding is limited to one or a few of the conformations. Parsons and co-workers (*37*) have previously given a rationale for this equilibrium based on the fact that the apparent on-rate constant for GST M1-1 is less than expected for a diffusion-limited process (Table 2). It could be argued that a mechanism where binding is restricted to a rare ionic form of glutathione could give a low apparent on-rate. However, a charged analogue of glutathione, glutathione sulfonate, displays the same association rate with rat GST M1-1 as does glutathione (*37*). In

Table 2: Preequilibrium Constants from Binding of Glutathione for GST A1-1 Mutants and Different GSTs[a]

			fluorescence measurements			absorption measurements			
enzyme	temp (°C)	pH	k_{on} (mM^{-1} s^{-1})	k_{off} (s^{-1})	K_D (μM)[b]	k_{on} (mM^{-1} s^{-1})	k_{off}^{app} (s^{-1})	K_D (μM)[b]	K_D (μM)[c]
hGST A1-1 wild-type	5	6.0	−[g]	−	−	570 ± 40	210 ± 20	370	300 ± 70
hGST A1-1 wild-type	5	6.25	−	−	−	400 ± 60	210 ± 30	530	190 ± 60
hGST A1-1 wild-type	5	6.5	420 ± 30	74 ± 15	180	420 ± 20	160 ± 10	380	170 ± 30
hGST A1−1 wild-type	5	6.75	460 ± 30	58 ± 27	130	530 ± 130	67 ± 33	130	130 ± 30
hGST A1-1 wild-type	5	7.0	ND[f]	ND	ND	450 ± 20	58 ± 12	130	190 ± 50
hGST A1-1 wild-type	5	7.25	430 ± 40	41 ± 34	100	380 ± 70	63 ± 25	170	100 ± 10
hGST A1-1 M208Kh	5	6.5	−	−	−	910 ± 310	190 ± 80	210	ND
hGST A1-1 M208Kh	5	7.0	−	−	−	750 ± 90	110 ± 30	150	ND
hGST A1-1 F220A	5	7.0	−	−	−	1170 ± 300	190 ± 80	160	ND
hGST A1-1 F220T	5	7.0	−	−	−	640 ± 30	210 ± 10	330	ND
hGST P1-1[d]	5	6.5	≥1000	30 ± 6	−	≥1000	30 ± 6	−	ND
rGST T2-2	4	7.5	0.45 ± 0.05	0.6 ± 0.1	1300	ND	ND	ND	ND
rGST M1-1[e]	25	7.0	−	−	−	4300 ± 200	111 ± 13	26 ± 3	ND

[a] Parameter values, in the present study, and their standard deviations were obtained by regression analysis. The error between the experiments was estimated to 15% for the WT, based on replicate experiments. [b] Calculated from the quotient between k_{off} and k_{on}. [c] Value derived from the saturation curve obtained when the amplitude at 239 nm was plotted against [GSH]. [d] From Caccuri et al. (*36*). [e] From Parsons et al. (*37*). [f] ND, data are not determined. [g] (−) Data could not be obtained.

Scheme 1

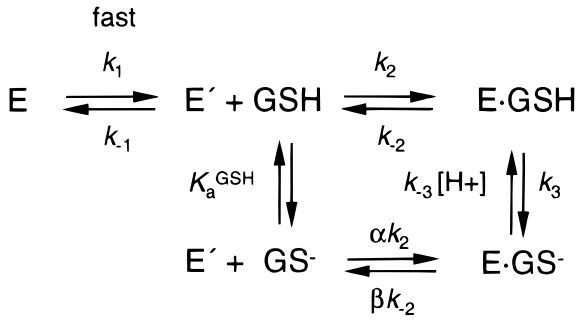

addition, the mutation F220A in GST A1-1, which does not alter the charge in the binding site, enhances the rate of glutathione binding. Therefore, such a restriction could not be the only cause of the slow binding. The increased binding rate of F220A (Table 2) also excludes that the substrate−enzyme association rate is reduced by charge repulsion between the substrate and the enzyme. Most likely, the association rate is limited by the access to the active site, which is dependent on the conformation of the mobile C-terminus of GST A1-1.

Glutathione probably binds to the enzyme both in the thiol and in the thiolate form. However, at the highest pH values used in this study, the concentration of thiol is more than 50 times higher than the concentration of the thiolate. To simplify the analysis of the present data, it is therefore assumed that the contribution from αk_2 to the apparent on-rate is negligible.

The quenching of fluorescence could only be measured at low glutathione concentrations where the observed rate constant for glutathione binding is described by a linear relationship derived from the general solution for the preequilibrium kinetics of two consecutive, reversible reaction steps (*38*):

$$k_{obs}^{fluores} = k_{-2}\frac{k_{-3}[H^+]}{k_3 + k_{-3}[H^+]} + \beta k_{-2}\frac{k_3}{k_3 + k_{-3}[H^+]} + k_2\frac{k_1[GSH]}{k_1 + k_{-1}} \quad (1)$$

As discussed above, the apparent on-rate constant, k_2^{app} (denoted k_{on} in Table 2), will be affected by the rapid equilibrium of the first step and k_2^{app} will be lower than the true k_2:

$$k_2^{app} = k_2\frac{k_1}{k_{-1} + k_1} \quad (2)$$

The apparent off-rate is dependent upon the equilibrium of the third step and is a measure of the parallel release of the protonated and deprotonated glutathione. The ratio between the two is governed by the pK_a value of active-site-bound glutathione. The quenching of intrinsic fluorescence could only be followed at pH values equal to or above 6.5.

The apparent observed rate constant, k_{obs}^{abs}, obtained when ionization of glutathione is monitored at 239 nm, is described by a hyperbolic function of [GSH] (*38*):

$$k_{obs}^{abs} = k_{-3}[H^+] + \beta k_{-2}\frac{k_3}{k_3 + k_{-3}[H^+]} + \frac{k_3[GSH]}{(k_{-2} + k_3)/k_2^{app} + [GSH]} \quad (3)$$

The curvature of the hyperbolic function could only be seen when the experiments were carried out at high pH values, i.e., >pH 6.75. At low pH values, measurements could only be conducted under experimental conditions corresponding to the linear part of the function, since the combination of a high proton concentration and a high glutathione concentration resulted in too large k_{obs} values. The rate constants for deprotonation of glutathione within the active site of the enzyme, k_3, obtained from the data at pH 6.75 and pH 7.25, were found to be 1500 ± 470 and 2940 ± 1360 s^{-1}, respectively. The experimental error is large, but k_3 exceeds 1000 s^{-1}. The experimental data collected from measurements at other pH values were subjected to linear regression analysis. The linear part is described by

$$k_{obs}^{abs} = k_{-3}[H^+] + \beta k_{-2}\frac{k_3}{k_3 + k_{-3}[H^+]} + \frac{k_2^{app}k_3[GSH]}{k_{-2} + k_3} \quad (4)$$

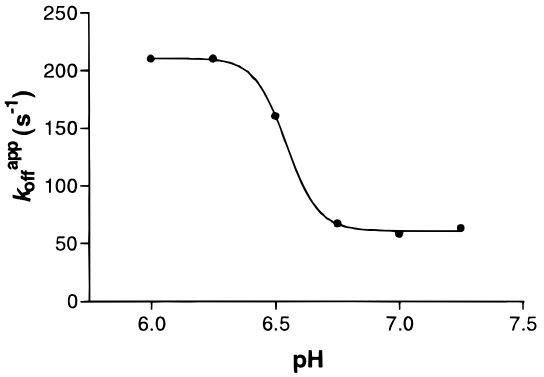

FIGURE 3: k_{off}^{app} values obtained from measurements of the active-site ionization of glutathione in wild-type GST A1-1, as a function of pH (eq 5).

The k_{-2} obtained when glutathione binding was measured by following the quenching of fluorescence was ~60 s^{-1} while k_3 is >1000 s^{-1}. Hence, the equation is simplified to

$$k_{obs}^{abs} = k_{-3}[H^+] + \beta k_{-2}\frac{k_3}{k_3 + k_{-3}[H^+]} + k_2^{app}[GSH] \quad (5)$$

The apparent on-rate, as for the on-rate obtained from the fluorescence measurements, reflects k_2^{app} (eq 2, denoted k_{on} in Table 2) while the apparent off-rate is a combination of the rate for reprotonation of glutathione within the G-site and the rate for release of deprotonated glutathione from the enzyme. The released glutathione is rapidly reprotonated by the buffer at the pH values used in the experiment. Consequently, the off-rate is a function of pH (Figure 3). At pH values well exceeding 6.7 (the pK_a of active-site-bound glutathione), the term $k_{-3}[H^+]$ is negligible, and the off-rate is limited by βk_{-2}. Equation 5 is based on the assumption that water is functioning as a proton donor when glutathione is protonated within the active site of the enzyme. If this is the case, the apparent off-rate obtained at pH values below the pK_a of glutathione should become a linear function of the proton concentration ($k_{off}^{app} = k_{-3}[H^+]$). However, as seen in Figure 3, the linear relationship is disrupted at pH values below approximately 6.4. This could indicate that active-site-bound glutathione is not protonated by water but is dependent on another titratable group, and that eq 5 should contain additional terms.

The apparent K_D value is 180 μM for the equilibrium between glutathione and wild-type GST A1-1 at pH 6.5 (Table 2), as calculated from the quotient of k_{off} and k_{on} obtained from the preequilibrium fluorescence measurements. The dissociation constant calculated from the experiments where ionization of glutathione has been monitored is a poor estimate of the true K_D value, since the apparent off-rate at low pH values is dependent on the protonation of glutathione within the active site (Scheme 1, eq 5, Figure 3). However, the values obtained from experiments conducted at high pH values agree well with the K_D from the quenching experiments. K_D values were also estimated from the saturation curves obtained by plotting the amplitude of glutathione ionization against the concentration of the tripeptide (Table 2).

The time-resolved active-site ionization of glutathione in the mutants was measured at pH 7.0. The apparent on-rate, k_2^{app} (denoted k_{on} in Table 2), is significantly enhanced for all the mutants. This implies that k_1 has increased in comparison with k_{-1} (eq 2) and that the equilibrium between the enzyme conformations in the step preceding glutathione binding has shifted toward E′ (Scheme 1).

Table 3: pK_a Values of Tyr9 in Wild-Type GST A1-1, M208Kh, and M208E and the pK_a Value of the Thiol Group of Enzyme-Bound Glutathione[a]

enzyme	pK_a(Tyr9)	pK_a(GSH)
wild type	8.2 ± 0.1	6.7 ± 0.1
M208E	7.9 ± 0.1	ND[b]
M208Kh	7.8 ± 0.1	6.5 ± 0.1
M208Kh + 4-PBA	8.1 ± 0.1	−[c]
F220A	7.8 ± 0.1	7.0 ± 0.1
F220T	7.9 ± 0.1	6.9 ± 0.1

[a] Parameter values and their standard deviation were obtained by nonlinear regression analysis. [b] ND, data are not determined. [c] (−) Data could not be obtained.

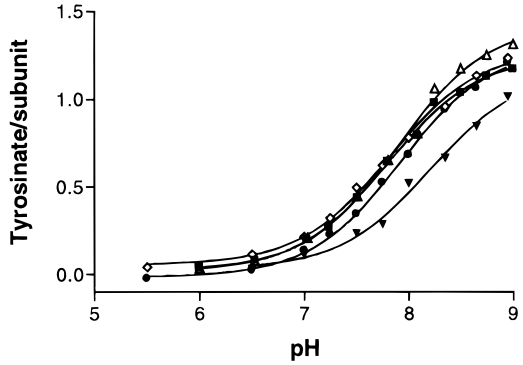

FIGURE 4: Titration of the tyrosinate formation in the active site of the GST A1-1 variants. The number of tyrosinates per subunit is plotted as a function of pH. (▼) Wild-type enzyme; (◇) M208Kh; (●) M208E; (■) F220A; (△) F220T. The pK_a values (Table 3) were obtained by fitting $\Delta A = \Delta A_{max}/[1 + 10^{(pK_a - pH)}]$ to the data.

As shown above, the apparent off-rate obtained is pH-dependent (eq 5). The pK_a of active-site-bound glutathione determines whether the measured rate is that of the release of glutathione thiolate from the active site (βk_{-2}) or the rate of reprotonation of glutathione within the active site ($k_{-3}[H^+]$). Since the pK_a of active-site-bound glutathione differs between the wild-type enzyme and the various mutants (Table 3), this complicates the comparison of the off-rates and the K_D values.

Determination of pK_a for Tyr9 and for Enzyme-Bound Glutathione. The ionization of the phenolic hydroxyl group of Tyr9 was monitored by UV absorption difference spectroscopy. Peaks corresponding to the deprotonation of Tyr9 were obtained at 298−301 and 250−255 nm, close to the wavelengths earlier ascribed to the formation of the tyrosinate (*13, 17*). The assignment was based on the mutation Y9F, which caused an elimination of these peaks at pH values below 9.0. The pK_a values are presented in Table 3. Differences between the values of the wild-type and the mutants are limited, but all the data points are independently measured and each point for the mutants shows a clear shift toward lower values. The pK_a value for wild-type GST A1-1 was similar to that earlier reported (*17*). The introduction of a charged amino acid in position 208 lowered the pK_a value of Tyr9 by approximately 0.3 pH unit (Figure 4, Table 3). Exchanging Phe220 for Ala or Thr caused a similar decrease. Binding of 4-propylbenzoic acid to the H-site of M208Kh

increased the pK_a value of Tyr9 (Table 3) to 8.1, which is close to the value of the wild-type enzyme.

The apparent pK_a value of the thiol group of enzyme-bound glutathione was determined by plotting the absorbance at 239 nm against pH (Table 3). The wild-type enzyme lowered the pK_a value of the thiol group from 9.2 in aqueous solution (*39*) to 6.7 in the active site. A pK_a of 6.6 has earlier been estimated indirectly from the kinetic pH profile of GST A1-1 (*17*) and from monitoring the formation of a σ-complex with 1,3,5-trinitrobenzene (*40*). A more basic pK_a value, 7.4, has been reported for the rat enzyme (*13*). The pK_a of the thiol group was slightly shifted toward a lower value by the M208K mutation (Table 3). In contrast, the F220 mutations raised the pK_a value of the thiolate to approximately 6.9.

DISCUSSION

The Alpha-class-specific C-terminal region of GST A1-1 (Figure 1) is mobile and adopts different conformations depending on the occupancy of the active site and the characteristics of the bound molecules (*25, 26*). Ligand binding apparently stabilizes a helical structure of the C-terminus. Mutant variants of GST A1-1 that have a decreased stability of the C-terminal helix have now been characterized to further explore the role of the C-terminus.

Preequilibrium Kinetics of Glutathione Binding. The apparent on-rate for glutathione binding to GST A1-1 is 450 mM^{-1} s^{-1}. The binding rate is lower than the diffusion-controlled value that could be expected for an enzyme−substrate association (*38*). The flexibility of the C-terminal region appears to be the best explanation to the binding data. The access of the active site is limited by the C-terminus, and only certain conformations give an active site opened enough for binding. This issue is more thoroughly discussed under Results.

Upon glutathione binding, the thiol group is deprotonated at a rate greater than 1000 s^{-1}. This value agrees well with the value that can be estimated from the pK_a values of water and glutathione and an approximated rate constant for protonation (*37*).

The pH dependence of k_{off}^{app} (Figure 3) indicates that active-site protonation of glutathione might be dependent on a titratable group other than water. At pH values below the pK_a of active-site-bound glutathione, k_{off}^{app} should become a linear function of the proton concentration if water assists as a proton donor (eq 5). However, empirical data in the present study show that the linearity breaks down at pH values below 6.4 (Figure 3). The proton donor could be located either on the enzyme or on glutathione, as suggested by Widersten and co-workers (*40*).

The K_D value of 180 μM (Table 2), obtained from the preequilibrium fluorescence measurements of glutathione binding at pH 6.5, is consistent with the K_D value (180−230 μM) earlier determined for the wild-type enzyme by monitoring the ionization of Tyr9 by its UV absorbance (*17, 40*).

When the rate constants for glutathione binding of different classes of the GST family are compared (Table 2), a large variation among the enzymes is detected. There is a 2-fold difference between the k_{on} determined for GST A1-1 and the k_{on} for GST P1-1 (*36*). The Theta-class enzyme rat GST T2-2, on the other hand, displays a much slower binding of glutathione (Table 2). In all crystal structures solved for different GSTs, glutathione binds with essentially the same backbone conformation (*24, 41*−*43*). The glutathione-binding domain and the contacts formed between glutathione and the G-site are well conserved during evolution of the various isoenzymes (*43*−*45*). The existing variations appear to be too small to account for the more than 1000-fold difference in k_{on} for glutathione binding between rat GST T2-2 and the human Pi-class GST P1-1 (Table 2). Instead, it probably reflects the more open active site of GST P1-1 as compared to GST T2-2. The glutathione-binding site of human GST T2-2 is closed by a long C-terminal helical extension (*43*) requiring large conformational changes in order to permit glutathione binding and release (*35*). The structure of the Pi-class enzyme does not include a helical lid over the active site and is therefore more exposed to its surrounding medium. The helix that covers the active site of GST A1-1 is shorter and more flexible than the Theta-class helix. Therefore, GST A1-1 binds glutathione faster than does GST T2-2 but slower than does GST P1-1. The active site of the Mu class GSTs is confined by two loops that, like the Alpha-class C-terminus, are flexible (*46*). The association constant for rat GST M1-1 was determined at 25 °C and at pH 7.0 (*37*). From temperature dependence measurements of GST T2-2, a decrease in the on-rate of 7−8 times was estimated for the temperature change from 25 to 5 °C (data not shown). The effect on the on-rate for GST M1-1 might not be as large, but a reasonable estimate of the rate constant at 5 °C should be 500−1000 mM^{-1} s^{-1}, similar to those of GST A1-1 and GST P1-1.

As for the GSTs of different classes, the glutathione-binding rates of the different GST A1-1 variants used in the present study seem to correlate with the accessibility of the active site. The M208Kh mutation almost doubles the rate constant for glutathione binding (Figure 2, Table 2). Since none of the glutathione-binding residues has been altered or affected, the most likely explanation is a further displacement of the C-terminal region from the active site, caused by unfavorable interactions between the hydrophobic face of the amphipatic helix and the introduced charge. This conformational change may open the entrance of the G-site, and glutathione can more easily diffuse into the binding site. The proposal of a more exposed active site of M208Kh is supported by earlier studies in which the mutant was shown to be more sensitive to ionic-strength-induced inhibition than the wild-type enzyme (*30*). The F220 mutants also display increased rates for glutathione binding (Figure 2, Table 2). The increase can be explained in a similar manner, where the deletion of the aromatic ring in the C-terminus removes one of the important interactions between the C-terminal helix, Tyr9, and the rest of the H-site. The equilibrium of different structures of the C-terminal region is consequently shifted toward more open conformations, which facilitate glutathione binding. It should be noted that the differences in on-rates are rather small and presumably correspond to small differences in structure.

Ionization of Active-Site Tyr9. The M208 and F220 mutations affected the ionization of Tyr9 in similar ways; the pK_a value was lowered from 8.2 in the wild-type enzyme to about 7.8−7.9 in the mutants (Figure 4, Table 3). For the M208 mutants, this difference has to be caused by some secondary effect since the phenolic hydroxyl group of Tyr9

is separated from the side chain in position 208 by 7.5 Å (Figure 1). The most probable cause of the lowered pK_a of Tyr9 is a more exposed active site since both the substitution of a polar side chain for Met208 and the deletion of the aromatic ring at position 220 are likely to perturb the conformation of the C-terminus. The lowered pK_a value of M208Kh can be raised to the wild-type value by addition of 4-propylbenzoic acid, the H-site-directed activator of M208Kh. The negative charge of the activator is believed to balance the positive charge of the lysine side chain and neutralize the unfavorable interaction between the C-terminus and the H-site (*30*).

The assumption that a dislocation of the C-terminal region could lower the pK_a value of Tyr9 contradicts the conclusions made by Atkins and co-workers (*28*), who found that ionization of Tyr9 was induced by pressure. They argued that increased pressure promotes the packing of the C-terminal helix against the active site, resulting in both a lowered pK_a of Tyr9 and a negative volume change of the system. The effect of pressure-induced ionization of Tyr9 was tested on wild-type rat GST A1-1 and on different mutants, F220Y, F220I, and F220L. For the wild-type enzyme, the value of $p_{1/2}$ (where 50% of Tyr9 was ionized) was 0.52 kbar while the two aliphatic substitutions made Tyr9 ionize at lower pressures; F220I and F220L displayed $p_{1/2}$ values of 0.41 and 0.46 kbar, respectively. For F220Y, higher pressures were needed in order to ionize Tyr9 ($p_{1/2}$ = 0.61 kbar). According to the authors' interpretation of the data, this would indicate that a lower pressure is needed in order to pack the C-terminal helix against Tyr9 in the F220I and F220L mutants. However, application of pressure in general leads to protein unfolding, which decreases the system volume (*47*). Thus, the raised pressure could instead cause an unfolding of the small proportion of the C-terminus that has a defined structure in the unliganded enzyme (*25*). The on-face hydrogen bond between Tyr220 and Tyr9 proposed by Dietze and co-workers (*27*) could stabilize the helix and protect it from pressure-induced perturbation, thus giving the high $p_{1/2}$ value. The F220L and F220I mutations probably decrease, rather than increase, the stability of the C-terminal region, and high pressures will make it even more disorganized. The insensitivity to pressure displayed by the binary *S*-methylglutathione−GST A1-1 complex can be explained by the stabilizing effect on the C-terminus afforded by the G-site ligand (*25, 26*). As for the F220 mutants used in the present study, the F220I and F220L mutants in rat GST A1-1 display a slightly decreased pK_a value (≈0.3 log unit) of Tyr9. Atkins and co-workers consider the possibility of pressure-induced destabilization of the helix, but they believe that Tyr9 is unlikely to maintain its unusually low pK_a value in the microenvironment of a more open active site. We propose that this is possible for small conformational changes of the C-terminal region.

Increased Nucleophilicity of the Thiolate Induced by Stabilization of the C-Terminal Helix? As pointed out, lowering the pK_a value of the glutathione thiol group is an important component of the catalytic action of the GSTs. Another factor that could be of significance for the activation of the cysteinyl thiolate of glutathione is desolvation of the negatively charged sulfur (cf. *48*). Kinetic isotope effects, measured in the reaction catalyzed by rat GST A1-1 (*49*), provided evidence for a mechanism involving thiolate desolvation as one important step. It appears likely that the nucleophilic tripeptide, together with the hydrophobic substrate, could induce its own desolvation by stabilizing the more structured conformation of the C-terminal helix. The hydrophobic amino acids in the H-site-facing part of the helix and the hydrophobic substrate are expected to repel the water molecules clustered around the negatively charged thiolate in the active site (Figure 1). The desolvation of the negatively charged sulfur atom will make it more prone to react.

In summary, the present investigation has shown that alteration of the H-site residue M208 affects parts of the enzyme that are distant from the immediate surroundings of the amino acid side chain. The rate of glutathione binding is increased, and the pK_a value of the catalytically important Tyr9 is lowered. Similar effects are obtained with two totally different mutations, F220A and F220T. The results suggest that the altered G-site features are caused by dislocation of the C-terminal region, leading to a more open active site.

ACKNOWLEDGMENT

We gratefully acknowledge valuable comments on the manuscript by Professor Alan R. Fersht, Cambridge University, U.K.

REFERENCES

1. Mannervik, B., Ålin, P., Guthenberg, C., Jensson, H., Tahir, M. K., Warholm, M., and Jörnvall, H. (1985) *Proc. Natl. Acad. Sci. U.S.A. 82*, 7202−7206.
2. Meyer, D. J., Coles, B., Pemple, S. E., Gilmore, K. S., Fraser, G. M., and Ketterer, B. (1991) *Biochem. J. 274*, 409−414.
3. Buetler, T. M., and Eaton, D. L. (1992) *Environ. Carcinog. Ecotoxicol. Rev. C10*, 181−203.
4. Meyer, D. J., and Thomas, M. (1995) *Biochem. J. 311*, 739−742.
5. Pemble, S. E., Wardle, A. F., and Taylor, J. B. (1996) *Biochem. J. 319*, 749−754.
6. Board, P. G., Baker, R. T., Chelvanayagam, G., and Jermiin L. S. (1997) *Biochem. J. 328*, 929−935.
7. Stenberg, G., Board, P. G., and Mannervik, B. (1991) *FEBS Lett. 293*, 153−155.
8. Kolm, R. H., Sroga, G. E., and Mannervik, B. (1992) *Biochem. J. 285*, 537−540.
9. Kong, K.-H., Takasu, K., Inoue, H., and Takahashi K. (1992) *Biochem. Biophys. Res. Commun. 184*, 194−197.
10. Liu, S., Zhang, P., Ji, X., Johnson, W. W., Gilliland, G. L., and Armstrong, R. N. (1992) *J. Biol. Chem. 267*, 4296−4299.
11. Manoharan, T. H., Gulick, A. M., Reinemer, P., Dirr, H. W., Huber, R., and Fahl, W. E. (1992) *J. Mol. Biol. 226*, 319−322.
12. Wang, R. W., Newton, D. J., Huskey, S.-E. W., McKeever, B. M., Pickett, C. B., and Lu, A. Y. H. (1992) *J. Biol. Chem. 267*, 19866−19871.
13. Atkins, W. M., Wang, R. W., Bird, A. W., Newton, D. J., and Lu, A. Y. H. (1993) *J. Biol. Chem. 268*, 19188−19191.
14. Karshikoff, A., Reinemer, P., Huber, R., and Ladenstein, R. (1993) *Eur. J. Biochem. 215*, 663−670.
15. Liu, S., Ji, X., Gilliland, G. L., Stevens, W. J., and Armstrong, R. N. (1993) *J. Am. Chem. Soc. 115*, 7910−7911.
16. Meyer, D. J., Xia, C., Coles, B., Chen, H., Reinemer, P., Huber, R., and Ketterer, B. (1993) *Biochem. J. 293*, 351−356.
17. Björnestedt, R., Stenberg, G., Widersten, M., Board, P. G., Sinning, I., Jones, A., and Mannervik, B. (1995) *J. Mol. Biol. 247*, 765−773.
18. Dietze, E. C., Wang, R. W., Lu, A. Y. H., and Atkins, W. M. (1996) *Biochemsitry 35*, 6745−6753.
19. Parsons, J. F., and Armstrong R. N. (1996) *J. Am. Chem. Soc. 118*, 2295−2296.

20. Wang, J., Barycki, J., and Colman, R. F. (1996) *Protein Sci. 5*, 1032−1042.
21. Xiao, G., Liu, S., Ji, X., Johnson, W. W., Chen, J., Parsons, J. F., Stevens, W. J., Gilliland, G. L., and Armstrong, R. N. (1996) *Biochemistry 35*, 4753−4765.
22. Thorson, J. S., Shin, I., Chapman, E., Stenberg, G., Mannervik, B., and Schultz, P. G. (1998) *J. Am. Chem. Soc. 120*, 451−452.
23. Mannervik, B., and Danielson, U. H. (1988) *CRC Crit. Rev. Biochem. 23*, 283−337.
24. Sinning, I., Kleywegt, G. J., Cowan, S. W., Reinemer, P., Dirr, H. W., Huber, R., Gilliland, G. L., Armstrong, R. N., Ji, X., Board, P. G., Olin, B., Mannervik, B., and Jones, T. A. (1993) *J. Mol. Biol. 232*, 192−212.
25. Cameron, A. D., Sinning, I., L'Hermite, G., Olin, B., Board, P. G., Mannervik, B., and Jones, T. A. (1995) *Structure 3*, 717−727.
26. Lian, L.-Y. (1998) *Cell. Mol. Life Sci. 54*, 359−362.
27. Dietze, E. C., Ibarra, C., Dabrowski, M. J., Bird, A., and Atkins, W. M. (1996) *Biochemistry 35*, 11938−11944.
28. Atkins, W. M., Dietze, E. C., and Ibarra, C. (1997) *Protein Sci. 6*, 873−881.
29. Widersten, M., Björnestedt, R., and Mannervik, B. (1994) *Biochemistry 33*, 11717−11723.
30. Gustafsson, A., and Mannervik, B. (1999) *J. Mol. Biol. 288*, 787−800.
31. Sanger, F., Nicklen, S., and Coulson, A. R. (1977) *Proc. Natl. Acad. Sci. U.S.A. 74*, 5463−5467.
32. Laemmli, U. K. (1970) *Nature 227*, 680−685.
33. Habig, W. H., Pabst, M. J., and Jakoby, W. B. (1974) *J. Biol. Chem. 249*, 7130−7139.
34. Graminski, G. F., Kubo, Y., and Armstrong, R. N. (1989) *Biochemistry 28*, 3526−3568.
35. Jemth, P., and Mannervik, B. (1999) *Biochemistry 38*, 9982−9991.
36. Caccuri, A. M., Lo Bello, M., Nuccetelli, M., Nicotra, M., Rossi, P., Antonini, G., Federici, G., and Ricci, G. (1998) *Biochemistry 37*, 3028−3034.
37. Parsons, J. F., Xiao, G., Gilliland, G. L., and Armstrong, R. N. (1998) *Biochemistry 37*, 6286−6294.
38. Fersht, A. (1999) *Structure and Mechanism in Protein Science. A Guide to Enzyme Catalysis and Protein Folding*, pp 132−168, W. H. Freeman & Co., New York.
39. Jung, G., Breitmaier, E., and Voelter, W. (1972) *Eur. J. Biochem. 24*, 438−445.
40. Widersten, M., Björnestedt, R., and Mannervik, B. (1996) *Biochemistry 35*, 7731−7742.
41. Armstrong, R. N. (1997) *Chem. Res. Toxicol. 10*, 2−18.
42. Koehler, R. T., Villar, H. O., Bauer, K. E., and Higgins, D. L. (1997) *Proteins: Struct., Funct., Genet. 28*, 202−216.
43. Rossjohn, J., McKinstry, W. J., Oakely, A. J., Verger, D., Flanagan, J., Chelvanayagam, G., Tan, K.-L., Board, P. G., and Parker, M. W. (1998) *Structure 6*, 309−322.
44. Armstrong, R. N. (1994) *Adv. Enzymol. Relat. Areas Mol. Biol.* 1−44.
45. Dirr, H., Reinemer, P., and Huber, R. (1994) *Eur. J. Biochem. 220*, 645−661.
46. Ji, X., Zhang, P., Armstrong, R. N., and Gilliland, G. L. (1992) *Biochemistry 31*, 10169−10184.
47. Frye, J. K., and Royer, C. A. (1998) *Protein Sci. 7*, 2217−2222.
48. Armstrong, R. N. (1991) *Chem. Res. Toxicol. 4*, 131−140.
49. Huskey, S.-E. W., Huskey, W. P., and Lu, A. Y. H. (1991) *J. Am. Chem. Soc. 113*, 2283−2290.

BI991482Y